Third order nonlinear optical property of Bi2Se3

Lu, Shunbin; Zhao, Chujun; Zou, Yanhong; Chen, Shuqing; Chen, Yu; Li, Ying; Zhang, Han; Wen, Shuangchun; Tang, Dingyuan

2013

Lu, S., Zhao, C., Zou, Y., Chen, S., Chen, Y., Li, Y., et al. (2013). Third order nonlinear optical property of Bi2Se3. Optics Express, 21(2), 2072-2082.

https://hdl.handle.net/10356/97548

https://doi.org/10.1364/OE.21.002072

Third order nonlinear optical property of Bi_2Se_3

Shunbin Lu,[1] Chujun Zhao,[1] Yanhong Zou,[1] Shuqing Chen,[1] Yu Chen,[1] Ying Li,[1] Han Zhang,[1,*] Shuangchun Wen,[1] and Dingyuan Tang[2]

[1]*Key Laboratory for Micro-/Nano-Optoelectronic Devices of Ministry of Education, College of Physics and Microelectronic Science, Hunan University, Changsha 410082, China*
[2]*School of Electrical and Electronic Engineering, Nanyang Technological University, Singapore 639798, Singapore*
**hanzhang@hnu.edu.cn*

Abstract: The third order nonlinear optical property of Bi_2Se_3, a kind of topological insulator (TI), has been investigated under femto-second laser excitation. The open and closed aperture *Z*-scan measurements were used to unambiguously distinguish the real and imaginary part of the third order optical nonlinearity of the TI. When excited at 800 nm, the TI exhibits saturable absorption with a saturation intensity of 10.12 GW/cm^2 and a modulation depth of 61.2%, and a giant nonlinear refractive index of 10^{-14} m^2/W, almost six orders of magnitude larger than that of bulk dielectrics. This finding suggests that the TI: Bi_2Se_3 is indeed a promising nonlinear optical material and thus can find potential applications from passive laser mode locker to optical Kerr effect based photonic devices.

OCIS codes: (160.4330) Nonlinear optical materials; (160.4236) Nanomaterials; (190.3270) Kerr effect; (190.7110) Ultrafast nonlinear optics.

References and Links

1. G. I. Stegeman, E. M. Wright, N. Finlayson, R. Zanoni, and C. T. Seaton, "Third order nonlinear integrated optics," J. Lightwave Technol. **6**(6), 953–970 (1988).
2. M. Dinu, F. Quochi, and H. Garcia, "Third-order nonlinearities in silicon at telecom wavelengths," Appl. Phys. Lett. **82**(18), 2954–2956 (2003).
3. M. Chattopadhyay, P. Kumbhakar, C. S. Tiwary, A. K. Mitra, U. Chatterjee, and T. Kobayashi, "Three-photon-induced four-photon absorption and nonlinear refraction in ZnO quantum dots," Opt. Lett. **34**(23), 3644–3646 (2009).
4. M. Chattopadhyay, P. Kumbhakar, R. Sarkar, and A. K. Mitra, "Enhanced three-photon absorption and nonlinear refraction in ZnS and Mn $^{2+}$ doped ZnS quantum dots," Appl. Phys. Lett. **95**(16), 163115 (2009).
5. Q. L. Bao, H. Zhang, Y. Wang, Z. Ni, Y. Yan, Z. X. Shen, K. P. Loh, and D. Y. Tang, "Atomic-Layer Graphene as a Saturable Absorber for Ultrafast Pulsed Lasers," Adv. Funct. Mater. **19**(19), 3077–3083 (2009).
6. H. Zhang, D. Y. Tang, L. M. Zhao, Q. L. Bao, and K. P. Loh, "Large energy mode locking of an erbium-doped fiber laser with atomic layer graphene," Opt. Express **17**(20), 17630–17635 (2009).
7. F. Bonaccorso, Z. Sun, T. Hasan, and A. C. Ferrari, "Graphene photonics and optoelectronics," Nat. Photonics **4**(9), 611–622 (2010).
8. Z. Sun, T. Hasan, F. Torrisi, D. Popa, G. Privitera, F. Wang, F. Bonaccorso, D. M. Basko, and A. C. Ferrari, "Graphene Mode-Locked Ultrafast Laser," ACS Nano **4**(2), 803–810 (2010).
9. A. Martinez, K. Fuse, B. Xu, and S. Yamashita, "Optical deposition of graphene and carbon nanotubes in a fiber ferrule for passive mode-locked lasing," Opt. Express **18**(22), 23054–23061 (2010).
10. Y. W. Song, S. Y. Jang, W. S. Han, and M. K. Bae, "Graphene mode-lockers for fiber lasers functioned with evanescent field interaction," Appl. Phys. Lett. **96**(5), 051122 (2010).
11. J. Sotor, G. Sobon, and K. M. Abramski, "Scalar soliton generation in all-polarization-maintaining, graphene mode-locked fiber laser," Opt. Lett. **37**(11), 2166–2168 (2012).
12. Z. Luo, M. Zhou, J. Weng, G. Huang, H. Xu, C. Ye, and Z. Cai, "Graphene-based passively Q-switched dual-wavelength erbium-doped fiber laser," Opt. Lett. **35**(21), 3709–3711 (2010).
13. J. Liu, S. Wu, Q. H. Yang, and P. Wang, "Stable nanosecond pulse generation from a graphene-based passively Q-switched Yb-doped fiber laser," Opt. Lett. **36**(20), 4008–4010 (2011).
14. J. L. Xu, X. L. Li, Y. Z. Wu, X. P. Hao, J. L. He, and K. J. Yang, "Graphene saturable absorber mirror for ultra-fast-pulse solid-state laser," Opt. Lett. **36**(10), 1948–1950 (2011).
15. Z. Zheng, C. Zhao, S. Lu, Y. Chen, Y. Li, H. Zhang, and S. Wen, "Microwave and optical saturable absorption in graphene," Opt. Express **20**(21), 23201–23214 (2012).
16. H. Zhang, S. Virally, Q. Bao, L. Kian Ping, S. Massar, N. Godbout, and P. Kockaert, "Z-scan measurement of the nonlinear refractive index of graphene," Opt. Lett. **37**(11), 1856–1858 (2012).
17. S. Yamashita, "A tutorial on nonlinear photonic applications of carbon nanotube and graphene," J. Lightwave Technol. **30**(4), 427–447 (2012).

#178635 - $15.00 USD Received 24 Oct 2012; revised 7 Dec 2012; accepted 14 Dec 2012; published 18 Jan 2013

18. X. L. Qi and S. C. Zhang, "Topological insulators and superconductors," Rev. Mod. Phys. **83**(4), 1057–1110 (2011).
19. M. Z. Hasan and C. L. Kane, "Colloquium: Topological insulators," Rev. Mod. Phys. **82**(4), 3045–3067 (2010).
20. F. Bernard, H. Zhang, S. P. Gorza, and P. Emplit, "Towards mode-locked fiber laser using topological insulators," in Nonlinear Photonics, OSA Technical Digest (online) (Optical Society of America, 2012), paper NTh1A.5.
21. C. Zhao, Y. Zou, Y. Chen, Z. Wang, S. Lu, H. Zhang, S. Wen, and D. Tang, "Wavelength-tunable picosecond soliton fiber laser with Topological Insulator: Bi_2Se_3 as a mode locker," Opt. Express **20**(25), 27888–27895 (2012).
22. C. Zhao, H. Zhang, X. Qi, Y. Chen, Z. Wang, S. Wen and D. Tang, "Ultra-short pulse generation by a topological insulator based saturable absorber," Appl. Phys. Lett. **101**(21), 211106 (2012).
23. J. Zhang, Z. P. Peng, A. Soni, Y. Y. Zhao, Y. Xiong, B. Peng, J. B. Wang, M. S. Dresselhaus, and Q. H. Xiong, "Raman spectroscopy of few-quintuple layer topological insulator Bi_2Se_3 nanoplatelets," Nano Lett. **11**(6), 2407–2414 (2011).
24. M. Sheik-Bahae, A. A. Said, T.-H. Wei, D. J. Hagan, and E. W. Van Stryland, "Sensitive measurement of optical nonlinearities using a single beam," IEEE J. Quantum Electron. **26**(4), 760–769 (1990).
25. R. A. Ganeev, A. I. Ryasnyansky, M. Baba, M. Suzuki, N. Ishizawa, M. Turu, S. Sakakibara, and H. Kuroda, "Nonlinear refraction in CS_2," Appl. Phys. B **78**(3–4), 433–438 (2004).
26. I. Moreels, Z. Hens, P. Kockaert, J. Loicq, and D. Van Thourhout, "Spectroscopy of the nonlinear refractive index of colloidal PbSe nanocrystals," Appl. Phys. Lett. **89**(19), 193106 (2006).
27. R. del Coso and J. Solis, "Relation between nonlinear refractive index and third-order susceptibility in absorbing media," J. Opt. Soc. Am. B **21**(3), 640–644 (2004).
28. M. Hajlaoui, E. Papalazarou, J. Mauchain, G. Lantz, N. Moisan, D. Boschetto, Z. Jiang, I. Miotkowski, Y. P. Chen, A. Taleb-Ibrahimi, L. Perfetti, and M. Marsi, "Ultrafast surface carrier dynamics in the topological insulator Bi_2Te_3," Nano Lett. **12**(7), 3532–3536 (2012).
29. J. A. Sobota, S. Yang, J. G. Analytis, Y. L. Chen, I. R. Fisher, P. S. Kirchmann, and Z. X. Shen, "Ultrafast optical excitation of a persistent surface-state population in the topological insulator Bi_2Se_3," Phys. Rev. Lett. **108**(11), 117403 (2012).
30. H. Zhang, C.-X. Liu, X.-L. Qi, X. Dai, Z. Fang, and S.-C. Zhang, "Topological insulators in Bi_2Se_3, Bi_2Te_3 and Sb_2Te_3 with a single Dirac cone on the surface," Nat. Phys. **5**(6), 438–442 (2009).
31. R. W. Boyd, S. G. Lukishova, and Y. R. Shen, *Self-focusing: Past and Present: Fundamentals and Prospect* (Springer, 2009), Chap. 24.

1. Introduction

Optical materials with a remarkably large third-order nonlinear susceptibility $\chi^{(3)}$, or a large *nonlinear refractive index* n_2, are highly in demand for all-optical signal processing applications, e.g. in ultra-short optical pulse shaper, optical switcher, wavelength converter, *etc* [1]. In the recent years, many materials had been experimentally confirmed to show large nonlinear refractive index. Conventional bulk semiconductors like GaAs and silicon possess a *nonlinear refractive index* $n_2 = 1.59 \times 10^{-17}$ m^2/W and $n_2 = 0.45 \times 10^{-17}$ m^2/W at telecom wavelengths, respectively [2]. For example, various quantum dots (QDs) studied at different wavelength: ZnO QDs at 1064 nm [3], ZnS QDs and Mn^{2+} doped ZnS QDs at 532nm wavelength [4]. In addition to these zero dimensional nano-materials, other 2-dimensional layer-by-layer new materials, such as graphene, were also experimentally found to show many interesting nonlinear optics properties. Unlike conventional bulk materials, the electrical and optical properties of few-layer materials can be effectively engineered over a wide spectral range by chemical or electrical doping, offering a great flexibility in tailoring their nonlinear optical characteristics. In addition, two-dimensional materials with layer geometry have also the intrinsic advantage of compatibility with the mature CMOS (complementary metal oxide semiconductor) technology. The imaginary part of the complex susceptibility in graphene, that is, saturable absorption term, has been widely investigated, and this property has led to the success in passive mode locking or Q-switching in lasers from visible band to microwave frequency band [5–15]. In the real part, large nonlinear refractive index $n_2 = 10^{-11}$ m^2/W was experimentally measured by Zhang *et al.* [16], making graphene promising for a number of photonic and optoelectronic applications [17].

In the parallel, the search for other new layered materials that have a comparable *nonlinear refractive index* is highly motivated. Another type of layer-by-layer material, the topological insulator (TI), has received great attentions in condensed-matter physics [18, 19]. TI is characterized by its bulk insulating state with a small band gap and a surface Dirac-like band structure, which is similar to that in graphene. Very recently, Bernard *et al.*

#178635 - $15.00 USD Received 24 Oct 2012; revised 7 Dec 2012; accepted 14 Dec 2012; published 18 Jan 2013

experimentally investigated the saturable absorption of topological insulator at the telecommunication [20] and Zhao *et al.* successfully used topological insulator as an effective saturable absorber for the passive mode locking of lasers [21, 22]. Enlightened by the similarity of electronic properties and saturable absorption between graphene and TI, one may wonder whether TI also has a large *nonlinear refractive index*.

In this paper, we present results of study on the *nonlinear refractive index* of a TI: Bi_2Se_3. Under femto-second laser illumination at the near-infrared wavelength region (800 nm), we measured the real and imaginary part of the complex *nonlinear refractive index* (saturable absorption and optical Kerr nonlinearity) with the laser *Z*-scan technique. At high optical intensity a clear saturation of the change in n_2 is observed. This may indicate large potentials of TI based nonlinear photonics devices for next-generation all-optical signal processing.

2. Experimental

2.1. Characterization of TI sample

By employing the polyol method reported in Ref [23], the Bi_2Se_3 nano-platelets (NPs) were synthesized, washed and dispersed in isopropyl alcohol (IPA) and dropped cast onto a common quartz plate (1 mm thick). After that, the quartz plate was put into a drying oven for evaporation over 8 hours. Figure 1(a) shows the Raman spectra of the as-produced Bi_2Se_3 sample, in which four typical Raman peaks attributed to different resonant modes could be clearly seen at low wave number range. Atomic force microscopy (AFM) was used to determine the sample thickness, as shown in Fig. 1(b). By scanning the height difference between the quartz substrate and the sample surface, the sample thickness is measured to be an average of 50 nm.

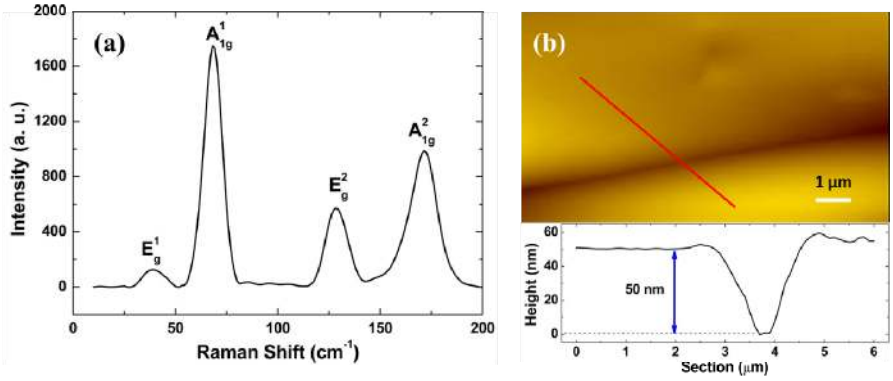

Fig. 1. Characterization of TI sample on quartz plate for *Z*-scan measurement. (a) Raman spectra of the TI sample. (b) The AFM image of the TI sample, the height between the black line and the others indicates approximately 50 nm for this batch of synthesis.

2.2. Experimental setup

The *Z*-scan technique was applied to study the nonlinear optics coefficients of the as-prepared TI: Bi_2Se_3. The experimental setup is shown in Fig. 2. The sample is subjected to femto-second pulses from a Coherent femto-second laser (center wavelength: 800 nm, pulse duration: 100 fs, 3 dB spectral width: 15 nm and repetition rate: 1 kHz). By using optical attenuators, the average power could be deliberately controlled below 1 mW, in order to ensure that the incident laser is adjusted below the optical damage threshold and the multiple-photon effect is significantly suppressed. The laser beam is then focused by an objective lens (focus length: 500 mm), generating a beam waist of 35 μm, corresponding to a peak intensity up to 260 GW/cm^2. The TI: Bi_2Se_3 sample was perpendicularly oriented towards the beam axis and translated along the *Z*-axis with a linear motorized stage. A computer controlled dual-detector power meters were used to simultaneously measure the optical power.

#178635 - $15.00 USD Received 24 Oct 2012; revised 7 Dec 2012; accepted 14 Dec 2012; published 18 Jan 2013

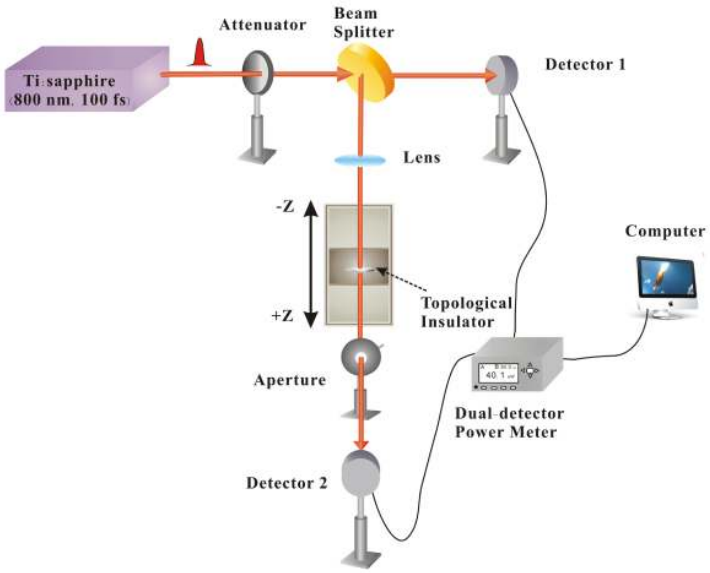

Fig. 2. Schematic diagram of the *Z*-scan experimental setup.

Measurements were performed simultaneously in two parts, an open-aperture part wherein all light transmitted through the sample is collected by the power-detector and a closed-aperture part wherein a small aperture is added before the power-detector so that only part of the on-axis transmitted beam is collected. The open-aperture measurement enables one to investigate the nonlinear absorption, while within the closed aperture measurement the change of optical transmittance is a combined consequence of the nonlinear absorption and the nonlinear phase effect induced by the optical Kerr nonlinearity. The division of the closed-aperture measurement by the open-aperture measurement results in the separation of these two effects [24]. To more precisely identify the *nonlinear refractive index*, CS_2 solution contained in a cuvette (1 mm in thick) was used as a benchmark for the calibration (see Appendix for details). Analyzing the measured *Z*-scan data, the third-order *nonlinear refractive index* of CS_2 is measured to be $n_2 = 2.66 \times 10^{-19}$ m^2/W, very close to the standard value of $(3 \pm 0.6) \times 10^{-19}$ m^2/W [25]. This result demonstrates the reliability of our *Z*-scan measurement platform.

3. Results and discussion

By replacing the standard CS_2 benchmark with the TI: Bi_2Se_3 sample while the other parameters were kept unchanged, *Z*-scan measurements on TI: Bi_2Se_3 were performed at an incident irradiance of 10.4 GW/cm^2, as shown in Fig. 3. A typical open aperture trace, when the sample is translated through the beam focus, is shown in Fig. 3(a). A sharp and narrow peak located at the beam focus clearly shows the characteristic of nonlinear absorption. A typical closed-aperture measurement was shown in Fig. 3(b). In this trace, as the effect of the nonlinear phase is of the same order of magnitude as the effect of saturable absorption, upon dividing the curve in Fig. 3(b) by the curve in Fig. 3(a), we could unambiguously verify the nonlinear phase change, as shown in Fig. 3(c). The latter has the typical shape of a *Z*-scan trace for Kerr nonlinearity. The pre-focal valley and the post-focal peak suggest the positive sign of the complex *nonlinear refractive index*, indicating the self-focusing effect in TI. Fitting the trace by the well-established formula [26],

#178635 - $15.00 USD Received 24 Oct 2012; revised 7 Dec 2012; accepted 14 Dec 2012; published 18 Jan 2013

$$T(x) = 1 + \frac{4x\Delta\Phi}{(1+x^2)(9+x^2)} + \frac{4(3x^2-5)\Delta\Phi^2}{(1+x^2)^2(9+x^2)(25+x^2)} + \frac{32(3x^2-11)x\Delta\Phi^3}{(1+x^2)^3(9+x^2)(25+x^2)(49+x^2)} \quad (1)$$

where, $T(x)$ is the normalized transmittance, $x = z / z_R$, $z_R = \pi\omega_0^2 / \lambda$, and $\Delta\Phi = kn_2 I_0 L_{eff}$ is the on-axis nonlinear phase shift at the focus, k is the wavelength number, I_0 is the irradiance at the focus, L_{eff} is the sample's effective length. The inferred nonlinear phase change $\Delta\Phi$ is about 1.1 rad and the real part of the complex *nonlinear refractive index* is calculated to be $n_2 = 2.26 \times 10^{-14}$ m^2/W.

Z-scan measurements under variable optical powers were also under investigation. Open-aperture measurement result shows that the normalized transmittance has a power dependent characteristic of saturable absorption. We fitted the curve in Fig. 4(a) by

$$T = 1 - \left(\frac{\alpha_s}{1 + I / I_{sat}} + \alpha_{ns}\right) \quad (2)$$

where, T is the transmittance, α_s is the saturable loss and α_{ns} is the non-saturable loss, I is the input intensity and I_{sat} is the saturation intensity. The fitted values of α_s and I_{sat} are 61.2% and 10.12 GW/cm^2, respectively. From the value of I_{sat}, we can calculate the nonlinear absorption coefficient that appears in Ref [27]. The high normalized modulation depth indicates that Bi_2Se_3 can be a suitable passive laser mode locker for the generation of ultra-short pulse.

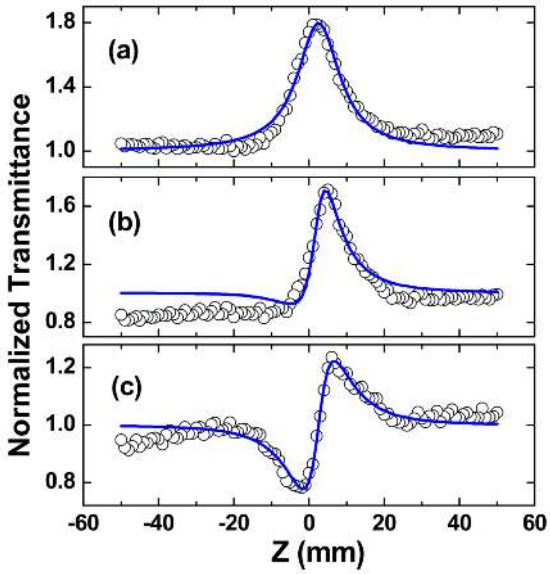

Fig. 3. *Z*-scan traces for Bi_2Se_3 sample at an average power of 40 μW, corresponding to a peak power at focus of 10.4 GW/cm^2. (a) Near field (open aperture). (b) Far field (closed aperture). Upon dividing by the near field curve one obtains the data of panel (c) which exhibits the typical shape of a *Z*-scan curve with positive nonlinear phase shift having an on-axis value of $\Delta\Phi = 1.1$ rad.

#178635 - $15.00 USD Received 24 Oct 2012; revised 7 Dec 2012; accepted 14 Dec 2012; published 18 Jan 2013

Figure 4(b) shows the nonlinear phase $\Delta\Phi$ under different input powers. The Kerr refractive index n_2 can be deduced from the slope of this curve at low intensities, based on $n_2 = \Delta\Phi / (k_0 LI)$, where $k_0 = 2\pi / \lambda$ and L is the sample thickness, assumed equal to 50 nm. A value of $n_2 \simeq 10^{-14}$ m^2/W is obtained, which is approximately 10^6 times larger than that of bulk dielectrics. With the laser intensity increasing, the nonlinear phase shift decreases and saturates starting from $I > I_{sat} \approx 50$ GW/cm^2. In this high intensity regime, a more accurate modeling of the nonlinear response taking into account $\chi^{(3)}$ and higher order terms, such as $\chi^{(5)}$. is required. However, from the experimental measurement, an effective nonlinear Kerr index could be defined by $n_2^* = \Delta\Phi / (k_0 LI)$, as a combined effect of *nonlinear refractive index* from different order terms. One sees that n_2^* decreases with increasing I and then reaches at a constant value $n_2^* = 10^{-14}$ m^2/W for $I_{sat} > 50$ GW/cm^2. Table1 shows the nonlinear refractive index of different optical materials and one could see that TI (Bi_2Se_3) has relatively large nonlinear refractive index, while TI (Bi_2Se_3) possesses the advantage of the two-dimensional geometry.

Table 1. Nonlinear Refractive Index n_2 of Different Materials

Material	λ, nm	Duration Time	n_2, m^2/W
GaAs	1540	220 fs	1.59×10^{-17} [a]
Si	1540	220 fs	0.45×10^{-17} [a]
ZnS QDs	532	10 ns	5.7×10^{-18} [b]
Mn^{2+} doped ZnS QDs	532	10 ns	6.8×10^{-18},8.6×10^{-18} [b]
ZnO QDs	1064	10 ns	1.7×10^{-18} [c]
Graphene	1550	3.8 ps	6×10^{-12} [d]
TI(Bi_2Se_3)	800	~100 fs	2.26×10^{-14} [e]
PbSe QDs	1200–1350	~100 fs	-3×10^{-15} ~-4×10^{-15} [f]

[a]From Appl. Phys. Lett. **82**, 2954-2956 (2003).
[b]From Appl. Phys. Lett. **95**, 163115 (2009).
[c]From Opt. Lett. **34**, 3644-3646 (2009).
[d]From Opt. Lett. **37**, 1856-1858 (2012).
[e]From the current work.
[f]From Appl. Phys. Lett. **89**, 193106 (2006).

The electronic property of TI is characterized by the bulk insulating band and surface Dirac-cone band [28–30]. In view of that the photon energy (1.55 eV) at 800 nm is larger than the bulk insulating band gap (0.3 eV) [29], the inter-band transitions (from the cone-like valence band into the conduction band) could occur. This is because that TI has symmetric energy band structure in its band state, the momentum conservation, as a result of electron excited from the conduction band to the valance band, could be automatically fulfilled, leading to a very broad spectral range of optical absorption. In principle, TI possesses broadband saturable absorption once the photon energy is larger than its bulk band gap, and operates as another broadband optical saturable absorber, like its counterpart: graphene.

#178635 - $15.00 USD Received 24 Oct 2012; revised 7 Dec 2012; accepted 14 Dec 2012; published 18 Jan 2013

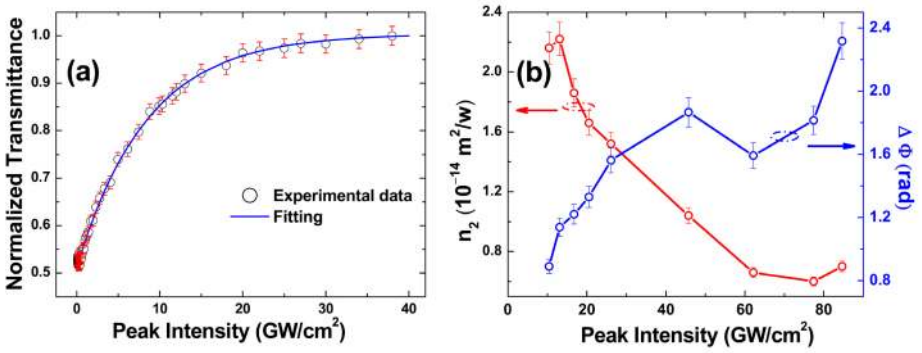

Fig. 4. (a) Relation between normalized transmittance and input peak intensity for Bi_2Se_3. (b) Dependence of ΔΦ (right axis) and n_2 (left axis) on peak intensity for Bi_2Se_3.

Furthermore, there are two main physical mechanisms responsible for the origin of nonlinear refraction: the bound-electronic and free-carrier nonlinearities [31]. The former effect is governed by $n(I) = n_0(I) + \Delta n(I) = n_0(I) + n_2 I$, while the latter follows $\Delta n(t) = n_2 I(t) + \sigma_\gamma N(t)$, where σ_γ is the free carrier refraction coefficient, and $N(t)$ is the photo-excited carrier density. We expect that these two mechanisms co-exist in the topological insulator material, and therefore, obviously, the *effective nonlinear Kerr index* $n_2^* = n_2 + \sigma_\gamma N(t)/I$ becomes an intensity dependent parameter, which can explain why n_2^* changes with the incident laser intensity in the experiments, as shown in Fig. 4(b). We correlate the origin of the large Kerr nonlinearity with the Dirac Fermions in the TI: Bi_2Se_3. At low power regime, the bound-electronic nonlinearity coexists with the free-carrier nonlinearity, as a result of a large amount of bound-electrons at the bulk conduction band and free-carriers at the surface metallic band; however with the increasing of the incident light, the depletion of electrons at the conduction band induced by the saturable absorption effect weakens the contribution from the bound-electronic nonlinearity, leading to the saturation of optical nonlinearity at the high power regime, as shown in Fig. 4(b). Consequently, if one reasonably assumes that only the free-carrier nonlinearity takes effect at the high power regime (I_{sat} >50 GW/cm^2), one can argue that *effective nonlinear Kerr index* from the free-carrier (resp. bound-electronic) nonlinearity is about to 0.8×10^{-14} m^2/W (resp. 1.4×10^{-14} m^2/W).

4. Conclusion

In conclusion, the third order nonlinear optics property in TI: Bi_2Se_3 was experimentally investigated by the open and closed aperture *Z*-scan technique, and its real and imaginary part of *nonlinear refractive index* (Kerr nonlinearity and saturable absorption) are separately determined, for the first time. Our measurements on the nonlinear phase and absorption yield a nonlinear coefficient n_2 of 10^{-14} m^2/W, a saturable intensity of 10.12 GW/cm^2 and a modulation depth of 61.2% at 800 nm under femto-second laser excitation. The measured value of the *effective nonlinear refractive index* decreases with increasing input power. Interestingly, it still remains large at the state of absorbance being saturated. This indicates that TI is highly favorable for the nonlinear optics application at high power regime (high nonlinear phase, low absorption).

More works are called for the investigation of the role of carrier dynamics in the slow time scale, and the value of *nonlinear refractive index* in the limit of defect-free topological insulators. It has been recently pointed out that the band-gap and Fermi energy level could be engineered in TI and the effect of band-gap tuning on the *nonlinear refractive index* remain unclear. More experiments with defect-free, thinner TI with controlled energy band structure will be required to further explore the third order nonlinear optics in the TI.

#178635 - $15.00 USD Received 24 Oct 2012; revised 7 Dec 2012; accepted 14 Dec 2012; published 18 Jan 2013

Appendix

A. Characterization of Bi_2Se_3 sample

Topological insulator (TI) is a new class of quantum matter for which its band structure of surface state is similar to that of graphene, and it has attracted great attention in condensed-matter physics. Bi_2Se_3 has been shown to be an ideal candidate for room-temperature topological insulating behavior as it has a band gap of 0.3 eV. We have synthesized the Bi_2Se_3 NPs with the method introduced in Ref [23], and the Raman spectrum and AFM image have determined the identity and measured the thickness of the sample, respectively. High quality NPs exhibit hexagonal morphologies with planar dimensions. Figure 5 shows the SEM images of chemically grown nanonplatelets (NPs). It can be seen that NPs exhibit hexagonal morphologies with planar dimensions that could extend up to several micrometers.

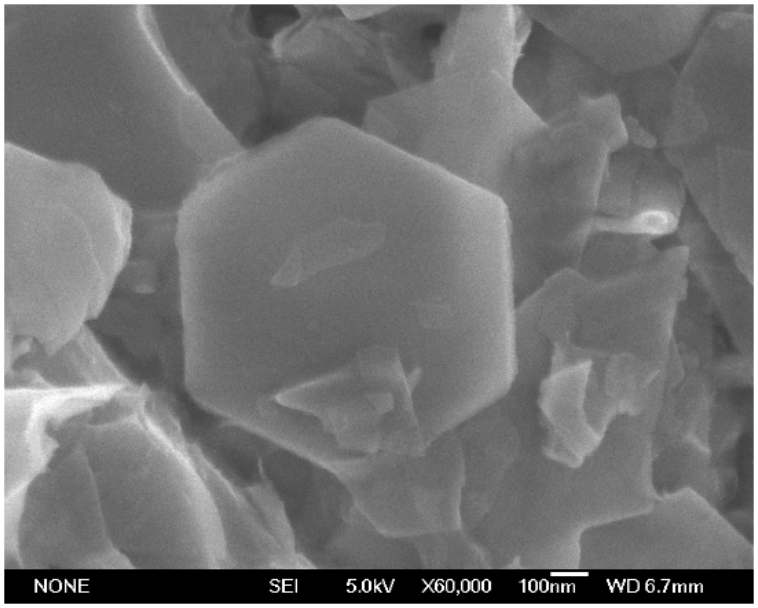

Fig. 5. SEM images of as-grown Bi_2Se_3 nanoplatelets.

B. Laser beam characterization

A CCD was used to measure the beam waist from a Coherent femto-second laser. Firstly, we ensure that after the focusing objective, the laser beam axis is perpendicular to the pin hole of the CCD, which is mounted upon the translation stage. Then, by finely adjusting the position of the beam profiler through the Newport M-ILS250CC linear motorized stage, the laser beam intensity distribution before and after the focus point can be captured by the CCD. Figure 6 shows a typical laser spectrum, the beam intensity profile, beam waist near the focus point and the relation between laser beam intensity and the relative position of the focus point. The laser beam waist near the focus point is measured to be as broad as 40 μm. The exact beam waist can be further inferred through fitting a typical *Z*-scan curve, which gives an estimated beam waist of 35 μm.

#178635 - $15.00 USD Received 24 Oct 2012; revised 7 Dec 2012; accepted 14 Dec 2012; published 18 Jan 2013

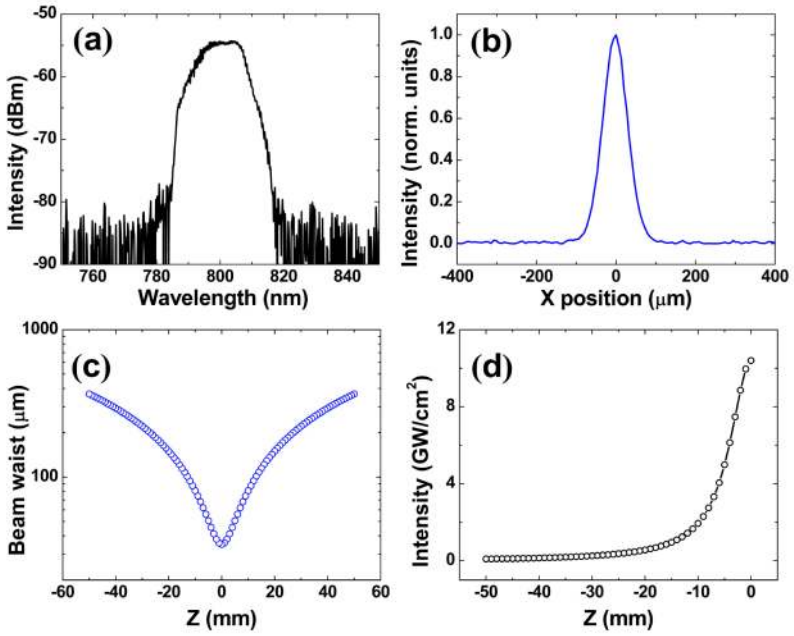

Fig. 6. (a) The optical spectrum of 800 nm laser. (b) Beam intensity profile near the focus point. (c) Relation between the beam waist and the relative position with respect to the focus point. (d) Relation between laser beam intensity and the relative position of the focus point for an optical input power of about 40 μW.

C. *Z*-scan measurement of CS_2 sample

CS_2 solution contained within a cuvette (1 mm in thickness) is deliberately used as a benchmark for calibration. Under the illumination of 76 GW/cm^2 intensity at the focus point, the *Z*-scan measurements to CS_2 sample are taken and the results are shown in the Fig. 7. From the Fig. 7 (a), we can see that the open aperture measurement has a typical curve of optical limiting effect, which indicates a two-photon absorption (2PA) effect. Due to the existence of the nonlinear absorption, the closed aperture measurement shown in Fig. 7(b) is asymmetric. Dividing by the open aperture curve, the Fig. 7(c) trace exhibits a typical shape of *Z*-scan curve. The nonlinear on-axis phase shift $\Delta\Phi$ is fitted to be 1.35 rad and the calculated *nonlinear refractive index* is about 2.66×10^{-19} m^2/W, which is in good agreement with $(3\pm0.6)\times10^{-19}$ m^2/W reported previously in Ref [25]. A plot of $\Delta\Phi$ versus peak laser irradiance as measured from various *Z*-scan on the same CS_2 cell is shown in Fig. 7(d). The linear behavior of this plot follows the theoretical model as derived for a cubic nonlinearity and the *nonlinear refractive index* n_2 becomes saturable. By comparing the experimentally measured nonlinear optics value on the standard CS_2 benchmark and the referenced value of CS_2 in Ref [25], we are able to conclude that our current measurement system is reliable and pulse duration still remains at a reasonable value around 100 fs after passing through many optical elements.

#178635 - $15.00 USD Received 24 Oct 2012; revised 7 Dec 2012; accepted 14 Dec 2012; published 18 Jan 2013

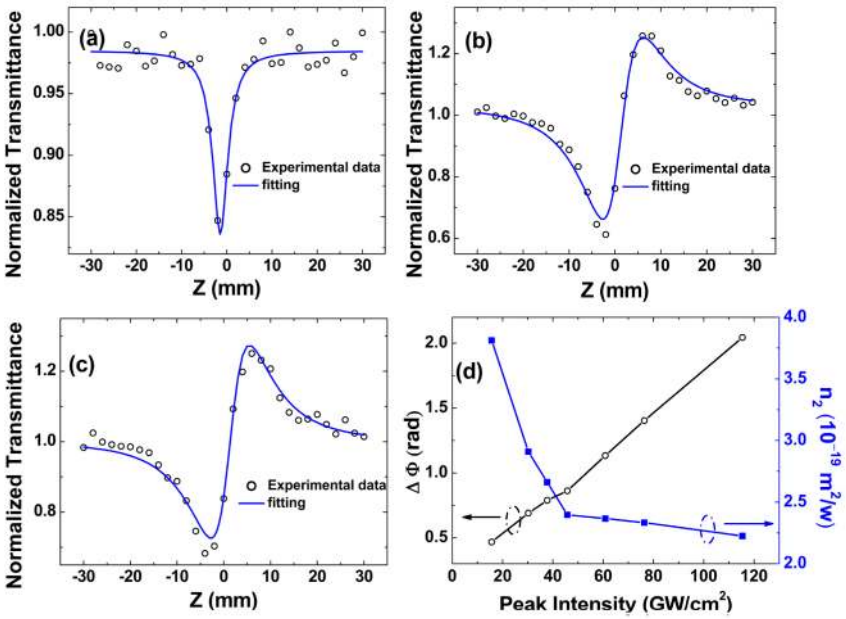

Fig. 7. *Z*-scan traces for 1 mm thickness CS_2 sample at a peak intensity of 76 GW/cm^2. (a) Near field (open aperture). (b) Far field (closed aperture). Upon dividing by the near field curve one obtains the data of panel (c) which exhibits the typical shape of a *Z*-scan curve with positive nonlinear phase shift having an on-axis value of $\Delta\Phi = 1.35$ rad. (d) The changes of $\Delta\Phi$ and n_2 with increasing peak intensity at the focus.

D. Fitting and calculation of the nonlinear refractive index

A closed aperture *Z*-scan trace shows the on-axis transmittance of the sample in the far field of a laser beam, when the sample is scanned through the focus of the beam. A sample with a *nonlinear refractive index* n_2 acts as a thin lens in this setup. For instance, a sample with positive n_2 will cause a divergence of the beam at pre-focal positions and a convergence at post-focal positions. This result is a typical valley-peak shape of the closed aperture trace (Fig. 8(b)). To calculate the on-axis phase shift $\Delta\Phi$, we used the Gaussian decomposition method, and expanded the calculations up to the third order in $\Delta\Phi$, as shown in Eq. (1). While the first order approximation is only allowed to determine small phase shifts, the third order approximation is valid up to $\Delta\Phi \approx 1.75$ [26].

To examine the effect of the quartz substrate, a pure quartz plate (1 mm in thickness) was taken as a reference for the open aperture and closed aperture measurement, at the intensity of 10.4 GW/cm^2. The results are shown in the Fig. 8, and we can see that the quartz sample has little change in normalized transmittance. In contrast with the curve of the Bi_2Se_3 sample, the substrate effect can be safely ignored. Using the third order approximation to fit the experimental data, the $\Delta\Phi \approx 1.1$ rad and the *nonlinear refractive index* is calculated to be $n_2 = 2.26\times10^{-14}$ m^2/W. Therefore, we could confirm that the peak-valley variation is only contributed by the third order nonlinear optics effect from the TI sample, and safely exclude the effect of the quartz substrate.

#178635 - $15.00 USD Received 24 Oct 2012; revised 7 Dec 2012; accepted 14 Dec 2012; published 18 Jan 2013

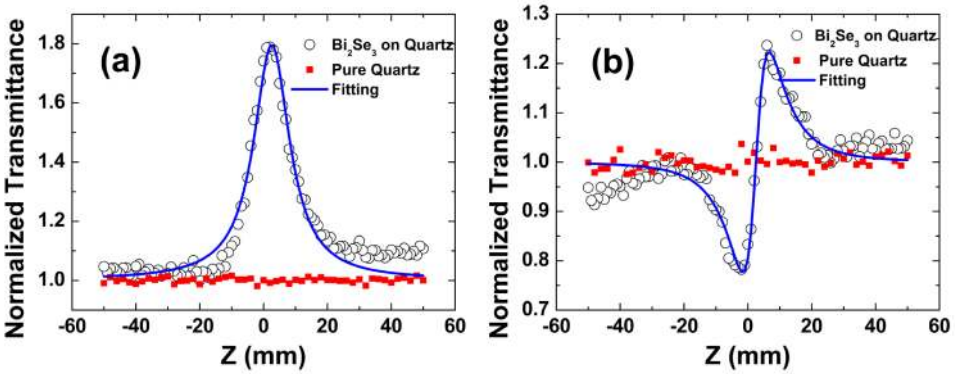

Fig. 8. *Z*-scan traces for Bi_2Se_3 sample and pure quartz plate at an average power of 40 μW, corresponding to a peak power at focus of 10.4 GW/cm^2. (a) Near field (open aperture). (b) Far field (closed aperture measurement/open aperture measurement).

Acknowledgment

This work is partially supported by the National 973 Program of China (Grant No. 2012CB315701), the National Natural Science Foundation of China (Grant Nos. 61025024 and 61205125), the National 863 Program of China (Grant No. 2011AA010203). Han ZHANG acknowledges the support from Program for New Century Excellent Talents in University of China (Grant No. NCET 11-0135), "Thousand Talents Program" for Distinguished Young Scholars and National Natural Science Fund Foundation of China for Excellent Young Scholars (Grant No. 61222505).